Coherent Interference Suppression with Complementally Transformed Adaptive Beamformer

Ta-Sung Lee and Tsui-Tsai Lin

***Abstract*— This paper proposes a beamforming scheme for suppressing coherent interference with an array of arbitrary geometry. The scheme first uses estimates of the source directions to construct a transformation, which removes the desired signal while retaining the coherent interference. Optimum beamforming is then performed on the transformed data containing only interference and noise to produce the maximum output signal-to-interference-plus-noise ratio (SINR). Analysis and numerical results demonstrate that the proposed complementally transformed beamformer significantly outperforms the conventional multiply constrained minimum variance (MCMV) beamformers.**

***Index Terms*— Adaptive arrays.**

I. Introduction

CONVENTIONAL adaptive beamformers are found to achieve high output SINR as long as the interferers are uncorrelated with the desired signal and the errors in the steering vector (due to pointing or calibration inaccuracy) are small [1]. In the presence of steering vector errors and/or correlated interferers, these beamformers exhibit severe degradation in performance. In some extreme cases, such as with a large pointing error or coherent interference (e.g. multipath interference), they break down as a result of desired signal cancellation. Remedies have been proposed to lessen the effect of desired signal cancellation [2]. In particular, the subtractive preprocessor [2] proves effective in improving the robustness against pointing errors for an adaptive beamformer operating on a uniform array. In spite of the success in dealing with a single correlated interferer, the subtraction preprocessed beamformer cannot handle multiple correlated interferers in general [3]. This is because that the array responses to the interferers are distorted by the subtractive preprocessor such that a mutual cancellation among the interferers cannot be effectively performed. To avoid such degradation, the spatial smoothing technique [4] can be incorporated as a means of decorrelating the interfering signals before beamforming. This ensures that the beamformer will effectively null each of the interferers instead of performing a mutual cancellation.

A major restriction of the subtractive preprocessing and spatial smoothing techniques is that they require a uniform array or an array consisting of several identical subarrays with which to operate. For the cases in which such array configurations cannot be obtained, other schemes must be employed to decouple the desired signal and coherent interference. In [5], a multiply constrained minimum variance (MCMV) beamformer was proposed, which suppressed coherent interferers by putting "hard nulls" in their hypothesized directions-of-arrival (DOA's). However, this approach is sensitive to errors in the DOA estimates. As an alternative, one can perform linear interpolation to convert a nonuniform array into a virtual uniform array [6]. To achieve a good beamforming performance, preliminary estimates of the source DOA's are again necessary for array interpolation. In general, the beamformer is more sensitive to the errors in the DOA estimates if the virtual array is more difficult to interpolate. That is, the success of the interpolated beamformers lies in that the original array must resemble some uniform array to a certain extent. Prior knowledge about the DOA's of the coherent interferers can be obtained by nonadaptive beamforming or other estimation methods [5] or by exploiting the geometrical features of the environment. For example, for above-sea communications the DOA of the multipath reflection can be estimated as the negative of the direct path DOA for a vertically deployed array.

This paper presents a new adaptive array processor for suppressing coherent interference with improved robustness to DOA estimation errors. The processor first employs a transformation to remove the desired signal and retain the coherent interference using the DOA estimates available. The transformation is constructed so as to minimize the difference between the original and transformed array data subject to the aforementioned "complemental constraints." The transformed data, which contain only the interference and noise, are then sent to a regular minimum variance distortionless response (MVDR) beamformer to compute the weight vector yielding the maximum output signal-to-interference-plus-noise ratio (SINR). Since the desired signal has been removed with the coherent interference retained, the optimum beamformer will try to perform a mutual cancellation for the coherent interferers solely. This is in contrast to the regular MVDR beamformer, which performs a mutual cancellation between the desired signal and coherent interferers. To verify the efficacy of the proposed complementally transformed minimum variance (CTMV) beamformer, a theoretical analysis is given to describe the behavior of the processor (including transformation and beamformer) in the presence of DOA estimation errors.

Manuscript received September 17, 1996; revised July 7, 1997. This work was supported by the National Science Council of R.O.C. under Grant NSC 85-2213-E-009-016.

The authors are with the Department of Communication Engineering, National Chiao Tung University, Hsinchu, Taiwan, R.O.C.

Publisher Item Identifier S 0018-926X(98)03365-1.

Simulations then follow to confirm the analysis results and demonstrate the advantages of the CTMV beamformer over the conventional MCMV beamformer.

II. Data Model and MCMV Beamformer

Some notations are defined below.

$(\cdot)^*$ Complex conjugate.
$(\cdot)^T$ Transpose.
$(\cdot)^H$ Complex conjugate transpose.
$\mathbf{0}_n$ $n \times 1$ zero vector.

A. Array Data Model

The scenario considered herein involves a single desired source, $J-1$ coherent interferers, and K uncorrelated interferers, all assumed to be narrowband with the same center frequency. These sources are in the far field of an array of M elements characterized by a known steering vector structure. Adopting the complex envelop notation, the array data obtained at a certain sampling instant can be put in the $M \times 1$ vector form

$$\begin{aligned}\boldsymbol{x} &= \sum_{i=1}^{J} s_i \boldsymbol{a}(\theta_i) + \sum_{i=J+1}^{J+K} s_i \boldsymbol{a}(\theta_i) + \boldsymbol{n} \\ &= \boldsymbol{A}_c \boldsymbol{s}_c + \boldsymbol{A}_u \boldsymbol{s}_u + \boldsymbol{n} \qquad (1)\end{aligned}$$

where

$$\begin{aligned}\boldsymbol{A}_c &= [\boldsymbol{a}(\theta_1), \boldsymbol{a}(\theta_2), \cdots, \boldsymbol{a}(\theta_J)] \\ \boldsymbol{A}_u &= [\boldsymbol{a}(\theta_{J+1}), \boldsymbol{a}(\theta_{J+2}), \cdots, \boldsymbol{a}(\theta_{J+K})] \qquad (2) \\ \boldsymbol{s}_c &= [s_1, s_2, \cdots, s_J]^T \\ \boldsymbol{s}_u &= [s_{J+1}, s_{J+2}, \cdots, s_{J+K}]^T. \qquad (3)\end{aligned}$$

The random scalars s_i, $i = 1, \cdots, J+K$ represent the source signals received at the reference point of the array. It is assumed that the first signal from direction θ_1 is the desired one. The $M \times 1$ vectors $\boldsymbol{a}(\theta_i)$, $i = 1, \cdots, J+K$ are the array steering vectors due to the $J+K$ sources. Finally, the vector $\boldsymbol{n}$ is composed of the complex envelops of the noise present at the M elements, which are assumed to be spatially white with power σ_n^2 and uncorrelated with all source signals.

B. MCMV Beamformers

The design of an MCMV beamformer for the above scenario involves minimizing the output power subject to the constraints that the desired signal receives a unit gain and the coherent interferers get rejected. Specifically, it determines the optimum weight vector $\boldsymbol{w}$ by solving the following optimization problem [5]:

$$\begin{aligned}&\min_{\boldsymbol{w}} \quad E\{|\boldsymbol{w}^H \boldsymbol{x}|^2\} \equiv \boldsymbol{w}^H \boldsymbol{R}_{xx} \boldsymbol{w} \\ &\text{subject to:} \quad \boldsymbol{w}^H \hat{\boldsymbol{A}}_c = \boldsymbol{f}^T \qquad (4)\end{aligned}$$

where $E\{\cdot\}$ denotes the expectation and $\boldsymbol{R}_{xx}$ is the $M \times M$ data correlation matrix defined by

$$\boldsymbol{R}_{xx} = E\{\boldsymbol{x}\boldsymbol{x}^H\} = \boldsymbol{A}_c \boldsymbol{R}_{sc} \boldsymbol{A}_c^H + \boldsymbol{A}_u \boldsymbol{R}_{su} \boldsymbol{A}_u^H + \sigma_n^2 \boldsymbol{I} \qquad (5)$$

with $\boldsymbol{R}_{sc} = E\{\boldsymbol{s}_c \boldsymbol{s}_c^H\}$ and $\boldsymbol{R}_{su} = E\{\boldsymbol{s}_u \boldsymbol{s}_u^H\}$ being the source correlation matrices involving the coherent sources and uncorrelated interferers, respectively. The noise correlation matrix is given by $\sigma_n^2 \boldsymbol{I}$ due to the spatial whiteness assumption, where $\boldsymbol{I}$ is the $M \times M$ identity matrix. In the constraint equation, $\hat{\boldsymbol{A}}_c$ is an estimate of $\boldsymbol{A}_c$ constructed with the DOA estimates for the coherent sources $\hat{\theta}_i$, $i = 1, \cdots, J$

$$\hat{\boldsymbol{A}}_c = [\boldsymbol{a}(\hat{\theta}_1), \boldsymbol{a}(\hat{\theta}_2), \cdots, \boldsymbol{a}(\hat{\theta}_J)] \qquad (6)$$

and

$$\boldsymbol{f} = \begin{bmatrix} 1 \\ \mathbf{0}_{J-1} \end{bmatrix}. \qquad (7)$$

The solution to (4) is given by [5]

$$\boldsymbol{w} = \boldsymbol{R}_{xx}^{-1} \hat{\boldsymbol{A}}_c (\hat{\boldsymbol{A}}_c^H \boldsymbol{R}_{xx}^{-1} \hat{\boldsymbol{A}}_c)^{-1} \boldsymbol{f}. \qquad (8)$$

III. Development of New Beamformer

The MCMV beamformer is generally sensitive to the errors in $\hat{\theta}_i$'s. To lessen the problem, high-order constraints can be incorporated to broaden the effective angular region of operation [5], [7]. Unfortunately, increasing the number of constraints results in poorer SINR performance since the effective degree of freedom for suppressing the uncorrelated interference and noise is reduced. Recently, the projection approach was proposed as a means of enhancing the SINR performance of the MCMV beamformer [8]. However, this type of beamformers can be applied only to uncorrelated interference scenarios.

A. Complemental Transformation

The aforementioned problems prompt the development of a beamformer, which does not require hard nulling for the coherent interferers. To work without hard nulling constraints, it is necessary to decouple the desired signal from other coherent interferers in order to avoid a mutual cancellation. By decoupling is meant that the desired signal is removed from the array data with other coherent interferers unchanged. This can be done with an $M \times M$ linear transformation $\boldsymbol{T}$ satisfying

$$\begin{aligned}\boldsymbol{T}\boldsymbol{a}(\theta_1) &= \mathbf{0}_M \\ \boldsymbol{T}\boldsymbol{a}(\theta_i) &= \boldsymbol{a}(\theta_i) \qquad i = 2, \cdots, J \qquad (9)\end{aligned}$$

such that

$$\boldsymbol{T}\boldsymbol{x} = \sum_{i=2}^{J} s_i \boldsymbol{a}(\theta_i) + \sum_{i=J+1}^{J+K} s_i \boldsymbol{T}\boldsymbol{a}(\theta_i) + \boldsymbol{T}\boldsymbol{n}. \qquad (10)$$

We refer to $\boldsymbol{T}$ as the complemental transformation since it performs the complemental function of the optimum beamformer, which removes the interferers with the desired signal retained. The complemental transformation is similar in principle to the subtractive preprocessor described in [2], which proved effective for alleviating desired signal cancellation. The restriction of the subtractive preprocessor, however, is that it can only be implemented on a uniform array.

Comparing (10) with (1) indicates that except for the desired signal, the only difference between them is the term involving the uncorrelated interference and noise. Thus, it is natural to see that in order for the beamformer to work properly with the transformed data $\boldsymbol{Tx}$, the remaining degree of freedom in $\boldsymbol{T}$ should be exploited to minimize the error

$$E\{\|\boldsymbol{Tx}-\boldsymbol{x}\|^2\} \equiv \text{tr}\{(\boldsymbol{T}-\boldsymbol{I})\boldsymbol{R}_{xx}(\boldsymbol{T}-\boldsymbol{I})^H\} \tag{11}$$

where $\|\cdot\|$ and $\text{tr}\{\cdot\}$ denote the vector two-norm and trace operator, respectively. Incorporation of the linear constraints of (9) in the minimization of (11) with θ_i's replaced by their estimates $\hat{\theta}_i$'s leads to the following constrained problem:

$$\min_{\boldsymbol{T}} \quad \text{tr}\{(\boldsymbol{T}-\boldsymbol{I})\boldsymbol{R}_{xx}(\boldsymbol{T}-\boldsymbol{I})^H\}$$
$$\text{subject to:} \quad \boldsymbol{T}\hat{\boldsymbol{A}}_c = \hat{\mathbf{B}}_c \tag{12}$$

where

$$\hat{\boldsymbol{B}}_c = [\mathbf{0}_M, \boldsymbol{a}(\hat{\theta}_2), \cdots, \boldsymbol{a}(\hat{\theta}_J)]. \tag{13}$$

B. Stability of T

It is noteworthy that the cost function in (12) implies that we are seeking a matrix $\boldsymbol{T}$ closest to $\boldsymbol{I}$ in terms of the generalized distance

$$d\{\boldsymbol{X},\boldsymbol{Y}\} = \sqrt{\text{tr}\{(\boldsymbol{X}-\boldsymbol{Y})\boldsymbol{R}_{xx}(\boldsymbol{X}-\boldsymbol{Y})^H\}} \tag{14}$$

under the constraints of (9). This makes sense because the ideal transformation, which maps each data vector into itself, is simply $\boldsymbol{I}$. Forcing $\boldsymbol{T}$ to be close to $\boldsymbol{I}$ also ensures better stability in that the transformation will be more robust to the errors in the DOA estimates for the coherent interferers ($\boldsymbol{Ia}(\theta) = \boldsymbol{a}(\theta)$ for all θ). However, stability problems can still arise if $\boldsymbol{R}_{xx}$ is ill conditioned, which typically occurs in the presence of a few strong sources. In this case, the distance in (14) becomes degenerate and the optimum $\boldsymbol{T}$ may no longer approximate $\boldsymbol{I}$. As a result, the transformation can be quite sensitive to the errors in $\hat{\boldsymbol{A}}_c$.

To remedy the sensitivity problem, $\boldsymbol{R}_{xx}$ should be modified into a better conditioned form. A simple method would be to add an auxiliary term $\lambda\boldsymbol{I}$ to decrease the effective signal-to-noise ratio (SNR) in $\boldsymbol{R}_{xx}$. The parameter λ should be chosen to be large enough to make the modified correlation matrix

$$\overline{\boldsymbol{R}}_{xx} = \boldsymbol{R}_{xx} + \lambda\boldsymbol{I} \tag{15}$$

sufficiently well conditioned but not too large to override the original signal/noise scenario in $\boldsymbol{R}_{xx}$. Detailed discussion about the selection of λ will be given shortly. Replacing $\boldsymbol{R}_{xx}$ with $\overline{\boldsymbol{R}}_{xx}$ in (12) and using the method of Lagrange multipliers, we obtain the minimizing $\boldsymbol{T}$ [9]

$$\boldsymbol{T} = \boldsymbol{I} - (\hat{\boldsymbol{A}}_c - \hat{\boldsymbol{B}}_c)(\hat{\boldsymbol{A}}_c^H\overline{\boldsymbol{R}}_{xx}^{-1}\hat{\boldsymbol{A}}_c)^{-1}\hat{\boldsymbol{A}}_c^H\overline{\boldsymbol{R}}_{xx}^{-1}. \tag{16}$$

C. High-Order Constraints

Another approach to enhancing the robustness of $\boldsymbol{T}$ against DOA estimation errors is to incorporate high-order derivative constraints in the directions of interest [7]. Specifically, with a set of Lth order constraints incorporated, the constraint equation in (12) can be extended to

$$\boldsymbol{T}\hat{\boldsymbol{A}}_c^{(m)} = \hat{\boldsymbol{B}}_c^{(m)}, \qquad m = 0, 1, \cdots, L \tag{17}$$

where

$$\hat{A}_c^{(m)} = [\boldsymbol{a}^{(m)}(\hat{\theta}_1), \boldsymbol{a}^{(m)}(\hat{\theta}_2), \cdots, \boldsymbol{a}^{(m)}(\hat{\theta}_J)]$$
$$\hat{\boldsymbol{B}}_c^{(m)} = [\mathbf{0}_M, \boldsymbol{a}^{(m)}(\hat{\theta}_2), \cdots, \boldsymbol{a}^{(m)}(\hat{\theta}_J)] \tag{18}$$

with

$$\boldsymbol{a}^{(m)}(\hat{\theta}_i) = \left.\frac{\partial^m \boldsymbol{a}(\theta)}{\partial\theta^m}\right|_{\theta=\hat{\theta}_i}, \qquad i = 1, 2, \cdots, J. \tag{19}$$

The expression of $\boldsymbol{T}$ with high-order constraints is identical to (16) except that $\hat{\boldsymbol{A}}_c$ and $\hat{\boldsymbol{B}}_c$ are replaced by the augmented matrices $[\hat{\boldsymbol{A}}_c, \cdots, \hat{A}_c^{(L)}]$ and $[\hat{\boldsymbol{B}}_c, \cdots, \hat{B}_c^{(L)}]$, respectively.

The major advantage of incorporating high-order constraints in the transformation stage instead of beamforming stage (as in MCMV beamformer) is that these constraints will not consume any degree of freedom of the optimum beamformer. Although working with (17) does indeed reduce the degree of freedom for minimizing the cost function in (12), it has relatively insignificant effects on the beamformer performance, as can be seen shortly in the simulation results.

D. Complementally Transformed Minimum Variance Beamformer

The optimum beamforming weight vector is determined via the MVDR criterion acting on the complementally transformed (CT) data $\boldsymbol{Tx}$

$$\min_{\boldsymbol{w}} \quad E\{|\boldsymbol{w}^H\boldsymbol{Tx}|^2\} \equiv \boldsymbol{w}^H\boldsymbol{T}\boldsymbol{R}_{xx}\boldsymbol{T}^H\boldsymbol{w}$$
$$\text{subject to:} \quad \boldsymbol{w}^H\boldsymbol{a}(\hat{\theta}_1) = 1. \tag{20}$$

Directly solving (20) raises two problems. First, $\boldsymbol{T}$ is not full rank such that the CT correlation matrix $\boldsymbol{TR}_{xx}\boldsymbol{T}^H$ is singular. Second, the noise component in $\boldsymbol{TR}_{xx}\boldsymbol{T}^H$ (which is $\sigma_n^2\boldsymbol{TT}^H$) is no longer the same as in the original $\boldsymbol{R}_{xx}$ (which is $\sigma_n^2\boldsymbol{I}$). These suggest that the CT correlation matrix be modified into a full rank matrix by replacing its noise part with $\sigma_n^2\boldsymbol{I}$

$$\tilde{\boldsymbol{R}}_{xx} = \boldsymbol{TR}_{xx}\boldsymbol{T}^H - \sigma_n^2\boldsymbol{TT}^H + \sigma_n^2\boldsymbol{I}. \tag{21}$$

Replacing $\boldsymbol{TR}_{xx}\boldsymbol{T}^H$ by $\tilde{\boldsymbol{R}}_{xx}$ and recognizing that (20) is a singly constrained version of (4), we obtain the complementally transformed minimum variance (CTMV) weight vector

$$\boldsymbol{w} = \frac{1}{\boldsymbol{a}^H(\hat{\theta}_1)\tilde{\boldsymbol{R}}_{xx}^{-1}\boldsymbol{a}(\hat{\theta}_1)}\tilde{\boldsymbol{R}}_{xx}^{-1}\boldsymbol{a}(\hat{\theta}_1). \tag{22}$$

E. Estimation of R_{xx} and σ_n^2

In practice, the true correlation matrix $\boldsymbol{R}_{xx}$ is usually estimated by its sample average version formed with a certain amount of data samples

$$\hat{\boldsymbol{R}}_{xx} = \frac{1}{N}\sum_{n=1}^{N}\boldsymbol{x}[n]\boldsymbol{x}^H[n] \tag{23}$$

where $\boldsymbol{x}[n]$ denotes the nth sample of the array data vector. On the other hand, the noise power σ_n^2 used for constructing $\tilde{\boldsymbol{R}}_{xx}$ can be estimated *a priori* by physical measurement or by numerical techniques. A popular technique is to compute the eigenvalues of $\hat{\boldsymbol{R}}_{xx}$ and identify those "smallest" eigenvalues

[10]. The effects of working with a finite sample size N and an erroneous estimate $\hat{\sigma}_n^2$ will be discussed shortly in the simulation section.

F. Algorithm Summary for CTMV Beamformer

The overall procedure of the CTMV beamformer can be summarized as below.

1) Obtain $\hat{\boldsymbol{R}}_{xx}$ and $\hat{\sigma}_n^2$.
2) Obtain DOA estimates for the desired source and coherent interferers.
3) Compute $\boldsymbol{T}$ according to (16) with $\boldsymbol{R}_{xx}$ replaced by $\hat{\boldsymbol{R}}_{xx}$ and λ given.
4) Compute $\tilde{\boldsymbol{R}}_{xx}$ according to (21) with $\boldsymbol{R}_{xx}$ and σ_n^2 replaced by $\hat{\boldsymbol{R}}_{xx}$ and $\hat{\sigma}_n^2$, respectively.
5) Compute $\boldsymbol{w}$ according to (22).

IV. Performance Analysis

In this section, we present analysis results on the CT steering vectors associated with the coherent sources and the output SINR of the CTMV beamformer. The scenario is simplified into that involving the desired source and a single coherent interferer only, i.e., $J = 2$ and $K = 0$. For the ease of expressions, the following notations are defined:

$$\begin{aligned} \sigma_i^2 &= E\{|s_i|^2\}; \quad \gamma_i = \frac{\sigma_i^2}{\sigma_n^2} \\ \eta_i &= \frac{\sigma_i^2}{\sigma_n^2+\lambda}, \qquad i=1,2 \end{aligned} \tag{24}$$

$$\begin{aligned} \boldsymbol{a}_i &= \boldsymbol{a}(\theta_i); \quad \hat{\boldsymbol{a}}_i = \boldsymbol{a}(\hat{\theta}_i) \\ \tilde{\boldsymbol{a}}_i &= \boldsymbol{T}\boldsymbol{a}(\theta_i), \qquad i=1,2 \end{aligned} \tag{25}$$

$$\rho = \frac{E\{s_1 s_2^*\}}{\sigma_1\sigma_2}; \quad \xi = \frac{\sigma_2}{\sigma_1} \tag{26}$$

$$\boldsymbol{a}_c = \boldsymbol{a}_1 + \rho^*\xi\boldsymbol{a}_2; \quad \tilde{\boldsymbol{a}}_c = \boldsymbol{T}\boldsymbol{a}_c \tag{27}$$

$$\begin{aligned} \mu_{ik} &= \frac{\boldsymbol{a}_i^H\boldsymbol{a}_k}{M}; \qquad \hat{\mu}_{ik} = \frac{\hat{\boldsymbol{a}}_i^H\hat{\boldsymbol{a}}_k}{M} \\ \tilde{\mu}_{ik} &= \frac{\tilde{\boldsymbol{a}}_i^H\tilde{\boldsymbol{a}}_k}{M}, \qquad i,k=1,2,c \\ \hat{\kappa}_{ik} &= \frac{\hat{\boldsymbol{a}}_i^H\boldsymbol{a}_k}{M}; \qquad \tilde{\kappa}_{ik} = \frac{\tilde{\boldsymbol{a}}_i^H\boldsymbol{a}_k}{M} \\ \tau_{ik} &= \frac{\tilde{\boldsymbol{a}}_i^H\hat{\boldsymbol{a}}_k}{M}, \qquad i,k=1,2,c. \end{aligned} \tag{28}$$

In (26)–(27), ρ denotes the correlation coefficient between the two coherent sources satisfying $|\rho| = 1$ and $\boldsymbol{a}_c$ represents the corresponding "composite" steering vector. Note that it is assumed that each of the array elements has an omnidirectional unit gain such that $||\boldsymbol{a}(\theta)||^2 = M$ for all θ.

Under the simplified scenario, the relevant quantities in (6), (13), (15), and (21) become

$$\hat{\boldsymbol{A}}_c = [\boldsymbol{a}(\hat{\theta}_1), \boldsymbol{a}(\hat{\theta}_2)]; \quad \hat{\boldsymbol{B}}_c = [\boldsymbol{0}_M, a(\hat{\theta}_2)] \tag{29}$$

$$\overline{\boldsymbol{R}}_{xx} = \sigma_1^2\boldsymbol{a}_c\boldsymbol{a}_c^H + (\sigma_n^2+\lambda)\boldsymbol{I}; \quad \tilde{\boldsymbol{R}}_{xx} = \sigma_1^2\tilde{\boldsymbol{a}}_c\tilde{\boldsymbol{a}}_c^H + \sigma_n^2\boldsymbol{I}. \tag{30}$$

A. CT Steering-Vector Error Analysis

In the first part, the effects of DOA estimation errors on the CT steering vectors $\tilde{\boldsymbol{a}}_i$, $i = 1, 2$, are analyzed. Only the main results will be given due to space limitation.

Substituting (29)–(30) in (16) and using the matrix inversion lemma, we obtain from (25) the CT steering vectors associated with the desired source and coherent interferer

$$\begin{aligned} \tilde{\boldsymbol{a}}_1 &= \boldsymbol{a}_1 - \frac{\hat{\kappa}_{11} - \hat{\mu}_{12}\hat{\kappa}_{21}}{(1-|\hat{\mu}_{12}|^2)}\hat{\boldsymbol{a}}_1 + \frac{M\eta_1}{1+\eta_1\delta} \\ &\quad \cdot \left[\mu_{c1} - \frac{\hat{\kappa}_{11}(\hat{\kappa}_{1c}^* - \hat{\mu}_{21}\hat{\kappa}_{2c}^*) + \hat{\kappa}_{21}(\hat{\kappa}_{2c}^* - \hat{\mu}_{12}\hat{\kappa}_{1c}^*)}{(1-|\hat{\mu}_{12}|^2)}\right]\hat{\boldsymbol{a}}_1 \\ \tilde{\boldsymbol{a}}_2 &= \boldsymbol{a}_2 - \frac{\hat{\kappa}_{12} - \hat{\mu}_{12}\hat{\kappa}_{22}}{(1-|\hat{\mu}_{12}|^2)}\hat{\boldsymbol{a}}_1 + \frac{M\eta_1}{1+\eta_1\delta} \\ &\quad \cdot \left[\mu_{c2} - \frac{\hat{\kappa}_{12}(\hat{\kappa}_{1c}^* - \hat{\mu}_{21}\hat{\kappa}_{2c}^*) + \hat{\kappa}_{22}(\hat{\kappa}_{2c}^* - \hat{\mu}_{12}\hat{\kappa}_{1c}^*)}{(1-|\hat{\mu}_{12}|^2)}\right]\hat{\boldsymbol{a}}_1 \end{aligned} \tag{31}$$

where

$$\begin{aligned} \delta = \frac{M}{1-|\hat{\mu}_{12}|^2}(\mu_{cc} + 2\,\mathrm{Re}\{\hat{\mu}_{21}\hat{\kappa}_{1c}\hat{\kappa}_{2c}^*\} \\ - \mu_{cc}|\hat{\mu}_{12}|^2 - |\hat{\kappa}_{1c}|^2 - |\hat{\kappa}_{2c}|^2) \end{aligned} \tag{32}$$

with $\mathrm{Re}\{\cdot\}$ denoting the real part. Two special cases $\hat{\theta}_2 = \theta_2$ ($\hat{\boldsymbol{a}}_2 = \boldsymbol{a}_2$) and $\hat{\theta}_1 = \theta_1$ ($\hat{\boldsymbol{a}}_1 = \boldsymbol{a}_1$) are considered below.

1) Perfect DOA Estimation for Coherent Interferer—$\hat{\boldsymbol{a}}_2 = \boldsymbol{a}_2$: In this case, we have from (28) $\hat{\mu}_{12} = \hat{\kappa}_{12}$, $\hat{\kappa}_{21} = \mu_{21}$, and $\hat{\kappa}_{2c} = \mu_{2c} = \mu_{21} + \rho^*\xi$. Substituting these in (31) along with the identities $\mu_{c1} = 1 + \rho\xi\mu_{21}$, $\mu_{cc} = 1 + \xi^2 + 2\xi\,\mathrm{Re}\{\rho\mu_{21}\}$, and $\hat{\kappa}_{1c} = \hat{\kappa}_{11} + \rho^*\xi\hat{\kappa}_{12}$, yields

$$\begin{aligned} \tilde{\boldsymbol{a}}_1 &= \boldsymbol{a}_1 - \frac{\hat{\kappa}_{11} - \mu_{21}\hat{\kappa}_{12}}{(1+\eta_1\delta)(1-|\hat{\kappa}_{12}|^2)}\hat{\boldsymbol{a}}_1 \\ \tilde{\boldsymbol{a}}_2 &= \boldsymbol{a}_2. \end{aligned} \tag{33}$$

As expected, the steering vector associated with the coherent interferer is perfectly retained according to (9).

In particular, $\tilde{\boldsymbol{a}}_1$ reduces to

$$\tilde{\boldsymbol{a}}_1 \approx \begin{cases} \boldsymbol{0}_M, & \text{for } \hat{\theta}_1 \approx \theta_1 \text{ and } \eta_1 \text{ small} \\ \boldsymbol{a}_1, & \text{for } \eta_1\delta \gg 1. \end{cases} \tag{34}$$

The first result follows from the facts that δ is small, $\hat{\kappa}_{11} \approx 1$, $\hat{\kappa}_{12} \approx \mu_{21}^*$, and $\hat{\boldsymbol{a}}_1 \approx \boldsymbol{a}_1$ for $\hat{\theta}_1 \approx \theta_1$. This says that the transformation is robust to a small error in $\hat{\theta}_1$ if the effective SNR η_1 is small. The second result indicates that the transformation fails to remove the desired source for a large error in $\hat{\theta}_1$ (for which δ is large) or a large η_1, yielding the trivial result of $\tilde{\boldsymbol{R}}_{xx} = \boldsymbol{R}_{xx}$. We thus see that in order for the transformation to work properly under a moderately small DOA estimation error, we should choose λ so that $\eta_1\delta$ is small relative to one. Since δ is no larger than M, a conservative guess would be $\lambda = M\sigma_1^2$ such that $\eta_1 < (1/M)$.

2) Perfect DOA Estimation for Desired Source—$\hat{\boldsymbol{a}}_1 = \boldsymbol{a}_1$: In this case, we have from (28) $\hat{\mu}_{21} = \hat{\kappa}_{21}$, $\hat{\kappa}_{12} = \mu_{12}$, and $\hat{\kappa}_{1c} = \mu_{1c} = 1 + \rho^*\xi\mu_{12}$. Substituting these in (31), along with the identities $\mu_{c2} = \mu_{12} + \rho\xi$, $\mu_{cc} = 1 + \xi^2 + 2\xi\,\mathrm{Re}\{\rho\mu_{21}\}$, and $\hat{\kappa}_{2c} = \hat{\kappa}_{21} + \rho^*\xi\hat{\kappa}_{22}$, yields

$$\begin{aligned} \tilde{\boldsymbol{a}}_1 &= \boldsymbol{0}_M \\ \tilde{\boldsymbol{a}}_2 &= \boldsymbol{a}_2 + \frac{1}{1+\eta_2\delta}\left(\rho\sqrt{\eta_1\eta_2}\delta + \frac{\hat{\kappa}_{21}^*\hat{\kappa}_{22} - \mu_{12}}{1-|\hat{\kappa}_{21}|^2}\right)\boldsymbol{a}_1. \end{aligned} \tag{35}$$

As expected, the steering vector associated with the desired source is removed, according to (9).

In particular, $\tilde{\boldsymbol{a}}_2$ reduces to

$$\tilde{\boldsymbol{a}}_2 \approx \begin{cases} \boldsymbol{a}_2, & \text{for } \hat{\theta}_2 \approx \theta_2 \text{ and } \eta_1\eta_2 \text{ small} \\ \boldsymbol{a}_2 + \dfrac{1}{\rho^*\xi}\boldsymbol{a}_1 = \dfrac{1}{\rho^*\xi}\boldsymbol{a}_c, & \text{for } \eta_2\delta \gg 1. \end{cases} \tag{36}$$

The first result follows from the facts that δ is small, $\hat{\kappa}_{22} \approx 1$, and $\hat{\kappa}_{21}^* \approx \mu_{12}$ for $\hat{\theta}_2 \approx \theta_2$. It says that the transformation is robust to a small error in $\hat{\theta}_2$ if $\eta_1\eta_2$ is small. The second result indicates that for a large error in $\hat{\theta}_2$ (for which δ is large) or a large η_2, $\boldsymbol{a}_2$ is transformed back into the composite steering vector in the absence of $\boldsymbol{a}_1$, leading again to the trivial result of $\tilde{\boldsymbol{R}}_{xx} = \boldsymbol{R}_{xx}$. In other words, the transformation performs a null operation by letting $\boldsymbol{a}_1$ reappear in $\tilde{\boldsymbol{R}}_{xx}$. Finally, similar to the previous argument, we find that an adequate value of λ for a reliable transformation is $\lambda = M\sigma_2^2$.

B. CTMV Beamformer Output SINR Analysis

In the second part, we present some main results on the analysis of the CTMV beamformer output SINR. The output SINR (denoted as SINR_o) is defined as the ratio of the output signal power P_s to the output interference-plus-noise power P_n. Since the interferer is coherent with the desired signal and there is no uncorrelated interference, the effective P_s and P_n are defined, respectively, as $P_s = \sigma_1^2|\boldsymbol{w}^H\boldsymbol{a}_c|^2$ and $P_n = \sigma_n^2\boldsymbol{w}^H\boldsymbol{w}$ [11].

Substituting (30) into (22) and using the matrix inversion lemma give the expanded form of the beamforming weight vector

$$\boldsymbol{w} = \hat{\boldsymbol{a}}_1 - \frac{M\gamma_1\tau_{c1}}{1 + M\gamma_1\tilde{\mu}_{cc}}\tilde{\boldsymbol{a}}_c \tag{37}$$

where we have omitted the constant gain in $\boldsymbol{w}$ since it does not affect the output SINR. Taking the ratio of P_s to P_n with the substitution of (37) yields the general expression for SINR_o

$$\text{SINR}_o = \frac{P_s}{P_n} = M\gamma_1 \cdot \frac{|\hat{\kappa}_{1c} + M\gamma_1(\tilde{\mu}_{cc}\hat{\kappa}_{1c} - \tilde{\kappa}_{cc}\tau_{c1}^*)|^2}{(1 + M\gamma_1\tilde{\mu}_{cc})^2 - M\gamma_1|\tau_{c1}|^2(2 + M\gamma_1\tilde{\mu}_{cc})} \tag{38}$$

where $\tilde{\mu}_{cc}$, $\tilde{\kappa}_{cc}$, and τ_{c1} are calculated by substituting (31) in (28). Again, two special cases are considered.

1) Perfect DOA Estimation for Coherent Interferer—$\hat{\boldsymbol{a}}_2 = \boldsymbol{a}_2$: In this case, SINR_o is given by (38) with $\tilde{\mu}_{cc}$, $\tilde{\kappa}_{cc}$, and τ_{c1} calculated by substituting (33) in (28).

Under the condition that $\hat{\theta}_1 \approx \theta_1$ and η_1 small, we have from (34) $\tilde{\mu}_{cc} \approx \xi^2$, $\tilde{\kappa}_{cc} \approx \xi^2 + \rho\xi\mu_{21}$, and $\tau_{c1} \approx \rho\xi\hat{\kappa}_{12}^*$ such that

$$\text{SINR}_o \approx M\gamma_1\frac{|\hat{\kappa}_{1c} + M\gamma_2(\hat{\kappa}_{1c} - \mu_{2c}\hat{\kappa}_{12})|^2}{(1 + M\gamma_2)^2 - M\gamma_2|\hat{\kappa}_{12}|^2(2 + M\gamma_2)} \tag{39}$$

which is the output SINR achieved in the "reliable mode" without severe desired signal cancellation. In particular, (39) reduces to

$$\text{SINR}_o \approx \begin{cases} M\gamma_1|\hat{\kappa}_{11}|^2, & \text{for } \hat{\kappa}_{12} \approx 0 \\ \approx M\gamma_1\dfrac{|\hat{\kappa}_{11} - \mu_{21}\hat{\kappa}_{12}|^2}{1 - |\hat{\kappa}_{12}|^2}, & \text{for } \gamma_2 \gg 1 \\ \approx M\gamma_1|\hat{\kappa}_{11} + \rho^*\xi\hat{\kappa}_{12}|^2, & \text{for } \gamma_2 \ll 1. \end{cases} \tag{40}$$

The first result indicates that as long as the coherent interferer is away from the mainlobe ($\hat{\kappa}_{12} \approx 0$), the CTMV beamformer performs like the optimum quiescent beamformer with the effect of pointing errors accounted for by $|\hat{\kappa}_{11}|$. The second and third results show the effects of a large and small γ_2, respectively, when the coherent interferer is close to the mainlobe ($\hat{\kappa}_{12} \approx 1$).

On the other hand, for $\eta_1\delta \gg 1$, we have from (34) $\tilde{\mu}_{cc} \approx \mu_{cc}$, $\tilde{\kappa}_{cc} \approx \mu_{cc}$, and $\tau_{c1} \approx \hat{\kappa}_{1c}^*$ such that

$$\text{SINR}_o \approx M\gamma_1\frac{|\hat{\kappa}_{1c}|^2}{1 + M\gamma_1(\mu_{cc} - |\hat{\kappa}_{1c}|^2)(2 + M\gamma_1\mu_{cc})} \tag{41}$$

which, as expected, is simply the output SINR achieved with the MVDR beamformer in the presence of pointing errors. In particular, (41) reduces to

$$\text{SINR}_o \approx \frac{|\hat{\kappa}_{11}|^2}{M\left(1 + \dfrac{\gamma_2}{\gamma_1}\right)(\gamma_1 + \gamma_2 - \gamma_1|\hat{\kappa}_{11}|^2)} \approx 0 \quad \text{for } \mu_{12} \approx 0 \text{ and } \gamma_i \gg 1, \qquad i = 1, 2 \tag{42}$$

which says that desired signal cancellation occurs when the coherent sources are strong and well separated ($\mu_{12} \approx 0$).

2) Perfect DOA Estimation for Desired Source—$\hat{\boldsymbol{a}}_1 = \boldsymbol{a}_1$: In this case, SINR_o is given by (38) with $\hat{\kappa}_{1c}$, $\tilde{\mu}_{cc}$, $\tilde{\kappa}_{cc}$, and τ_{c1} calculated by substituting (35) in (28).

Under the condition that $\hat{\theta}_2 \approx \theta_2$ and $\eta_1\eta_2$ small, we have from (36) $\hat{\kappa}_{1c} = \mu_{1c}$, $\tilde{\mu}_{cc} \approx \xi^2$, $\tilde{\kappa}_{cc} \approx \xi^2 + \rho\xi\mu_{21}$, and $\tau_{c1} \approx \rho\xi\mu_{12}^*$. It follows by a straightforward comparison that the corresponding SINR_o, achieved without pointing errors, is simply given by (39) with $\hat{\kappa}_{1c}$ and $\hat{\kappa}_{12}$ replaced by μ_{1c} and μ_{12}, respectively.

On the other hand, for $\eta_2\delta \gg 1$, we have from (36) $\hat{\kappa}_{1c} = \mu_{1c}$, $\tilde{\mu}_{cc} \approx \mu_{cc}$, $\tilde{\kappa}_{cc} \approx \mu_{cc}$, and $\tau_{c1} \approx \mu_{1c}^*$. Again, we see that the corresponding SINR_o is given by (41) with $\hat{\kappa}_{1c}$ replaced by μ_{1c}.

V. Computer Simulations

Computer simulations were conducted to ascertain the performance of the proposed CTMV beamformers. The array employed was a 20-element nonuniform linear array with the following interelement spacings (in terms of wavelength):

$$\{0.19, 0.19 \times 1.1, 0.19 \times 1.1^2, \cdots, 0.19 \times 1.1^{18}\}$$

which form a geometric sequence with the ratio 1.1. The parameters were chosen such that the array aperture is equal to 9.5 wavelengths corresponding to a uniform array with a halfwavelength spacing. All elements were assumed identical and omnidirectional with a unit gain. The scenario involved a desired source at $\theta_1 = 0°$ with power $\sigma_1^2 = 1$, a coherent

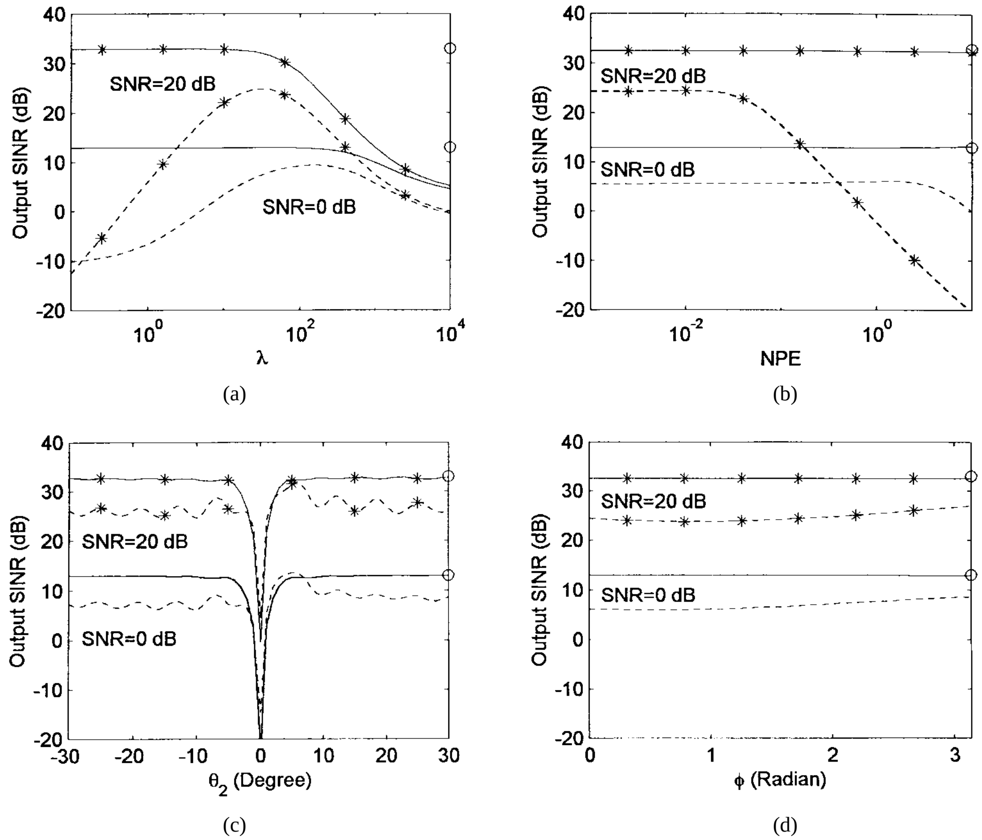

Fig. 1. Effects of λ, $\hat{\sigma}_n^2$, θ_2, and ϕ on CTMV beamformer. (a) Output SINR versus λ: $\hat{\sigma}_n^2 = \sigma_n^2$, $\theta_2 = 20°$, $\phi = 0$. (b) Output SINR versus $\hat{\sigma}_n^2$: $\lambda = 20$, $\theta_2 = 20°$, $\phi = 0$. (c) Output SINR versus θ_2: $\lambda = 20$, $\hat{\sigma}_n^2 = \sigma_n^2$, $\phi = 0$. (d) Output SINR versus ϕ: $\lambda = 20$, $\hat{\sigma}_n^2 = \sigma_n^2$, $\theta_2 = 20°$. Solid line with asterisk: SNR = 20 dB, $E_d = E_c = 0°$; dashed line with asterisk: SNR = 20 dB, $E_d = E_c = 2°$; solid line: SNR = 0 dB, $E_d = E_c = 0°$; dashed line: SNR = 0 dB, $E_d = E_c = 2°$; small circles: optimum SINR.

interferer at θ_2 (variable) with power $\sigma_2^2 = 1$, and an uncorrelated interferer at $\theta_3 = -45°$ with power $\sigma_3^2 = 100$ $(\text{SIR} = -20$ dB).

Unless otherwise mentioned, the set of "standard parameters"

$$\begin{aligned} &\lambda = M\sigma_1^2 = 20; \quad \hat{\sigma}_n^2 = \sigma_n^2; \quad \theta_2 = 20° \\ &\rho = e^{j\phi} = 1; \quad \hat{\boldsymbol{R}}_{xx} = \boldsymbol{R}_{xx} \end{aligned} \tag{43}$$

will be used throughout the section. Also, for the ease of presentation, the shorthand notations are defined

$E_d = \hat{\theta}_1 - \theta_1$: error of DOA estimate for desired source

$E_c = \hat{\theta}_2 - \theta_2$: error of DOA estimate for coherent interferer.

The simulations are organized in two parts. First, the general behaviors of the CTMV beamformer are examined. Second, the performance of the CTMV beamformer is compared with the MCMV beamformer for cases of zeroth and second order constraints. As an index of evaluation, the input SNR and output SINR were defined as

$$\text{SNR} \equiv \gamma_1 = \frac{\sigma_1^2}{\sigma_n^2}$$
$$\text{SINR}_o = \frac{\sigma_1^2 |\boldsymbol{w}^H \boldsymbol{a}_c|^2}{\sigma_3^2 |\boldsymbol{w}^H \boldsymbol{a}(\theta_3)|^2 + \sigma_n^2 \boldsymbol{w}^H \boldsymbol{w}}.$$

A. Part 1—General Behaviors of CTMV Beamformer

In the first set of simulations, we investigate the effects of λ, $\hat{\sigma}_n^2$ [noise-power estimate (NPE)], θ_2, and the phase ϕ of the correlation coefficient ρ on the output SINR performance of the CTMV beamformer with SNR and (E_d, E_c) as parameters. The results, obtained with the zeroth order $(L = 0)$ constraints, are given in Fig. 1. In each plot, four curves are shown. Those with and without asterisks correspond to the results obtained with SNR $= 20$ dB and SNR $= 0$ dB, respectively. On the other hand, the solid lines and dashed lines represent the results obtained with $(E_d, E_c) = (0°, 0°)$, and $(E_d, E_c) = (2°, 2°)$, respectively. The small circles on the right margin mark the maximum SINR values achievable with the optimum beamformer for SNR $= 20$ and 0 dB. Note that in each case, one of the parameters is varied and the others are fixed given by the standard setting in (43).

First, Fig. 1(a) shows the output SINR versus λ. It demonstrates that without DOA estimation errors, the beamformer performs reliably approaching the maximum SINR for a moderately small λ. In the presence of DOA estimation errors, however, a proper choice of λ is critical for the beamformer. Note that the acceptable range in this case is about $10 < \lambda < 100$, which confirms our assertion that a good choice is $\lambda = M\sigma_1^2 = 20$. For a large λ, the beamformer suffers some degradation due to the fact that the steering vector associated with the uncorrelated interferer

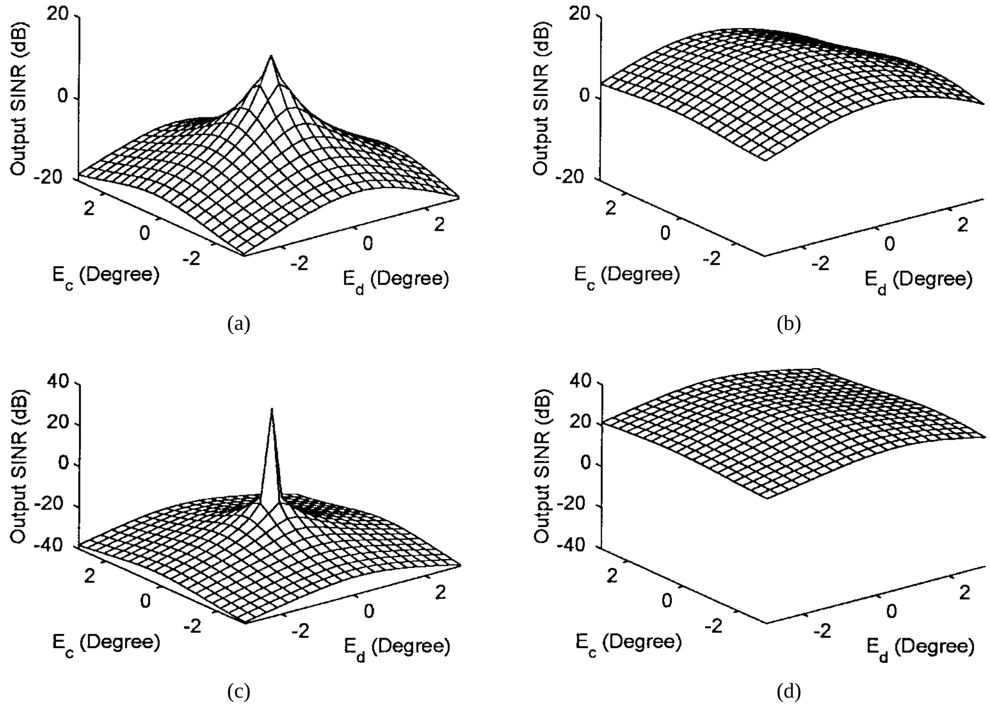

Fig. 2. Comparison of output SINR versus (E_d, E_c) for MCMV and CTMV beamformers employing zeroth order constraints. (a) MCMV, SNR $= 0$ dB. (b) CTMV, SNR $= 0$ dB. (c) MCMV, SNR $= 20$ dB. (d) CTMV, SNR $= 20$ dB.

was not successfully transformed. This is because that the transformation put less emphasis on the uncorrelated interferer when the "pseudo"noise power λ was increased.

To investigate the effects of noise correlation replacement in (21), the output SINR versus noise power estimate NPE is shown in Fig. 1(b). The results indicate that a right choice for $\hat{\sigma}_n^2$ (0.01 for SNR $= 20$ dB and 1 for SNR $= 0$ dB) is critical for the beamformer working in the presence of DOA estimation errors. The severe degradation occurring with an excessively large $\hat{\sigma}_n^2$ is, of course, due to the distortion of the signal/noise scenario in $\tilde{\boldsymbol{R}}_{xx}$.

Next, the DOA θ_2 of the coherent interferer is varied from $-30°$ to 30° and the corresponding output SINR values are plotted in Fig. 1(c). We see that the CTMV beamformer performs reliably as long as the coherent interferer is not too close to the mainlobe. For $\theta_2 \approx \theta_1 = 0°$, the beamformer breaks down even with perfect DOA estimates. This is because that the null associated with the coherent interferer causes severe distortion of the mainlobe such that the desired signal cannot be effectively received.

Finally, Fig. 1(d) shows the output SINR versus the phase ϕ of the correlation coefficient ρ between the desired source and coherent interferer. The results confirm that the CTMV beamformer can always suppress the coherent interferer, regardless of its phase relative to the desired source.

B. Part 2—Performance Comparison with MCMV Beamformer

In the second set of simulations, the performance of the CTMV beamformer is evaluated against DOA estimation errors and sample size N with the zeroth or second order $(L = 2)$ constraints employed for both the desired source and coherent interferer. For comparison, we also include the results obtained with the MCMV beamformer for which the high order constraints are chosen to be those with "conventional beamformer response" [7]. The standard setting in (43) was used for all cases except for the results in Fig. 4.

In Fig. 2, the three-dimensional plots of the output SINR against (E_d, E_c) are given for SNR $= 0$ and 20 dB with the zeroth order constraints employed. Clearly, the CTMV beamformer is much more robust to DOA estimation errors than the MCMV beamformer, especially at high SNR. The MCMV beamformer is quite sensitive to DOA estimation errors at high SNR due to severer desired signal cancellation. This problem is greatly alleviated by using the second-order constraints, as can be seen in Fig. 3. With the broader angular region offered by the high-order constraints, both beamformers gain improvements in the robustness against DOA estimation errors. Nevertheless, the MCMV beamformer is still significantly poorer than the CTMV beamformer in that the effective angular region of tolerance is small at high SNR.

To investigate the convergence behaviors of the two beamformers, we use the sample correlation matrix defined in (23) for computing the weight vectors and plot the output SINR against the sample size N in Fig. 4 for the ideal case of $(E_d, E_c) = (0°,\ 0°)$. Again, both the zeroth- and second-order constraints are tried. In each plot, the curves with and without asterisks correspond to the results obtained with SNR $= 20$ dB and SNR $= 0$ dB, respectively, and the solid lines and dashed lines represent the results obtained with the CTMV and MCMV beamformers, respectively. As expected, the output SINR increases as the number of samples increases. For both types of constraints, the CTMV beamformer converges much faster than the MCMV beamformer approaching the

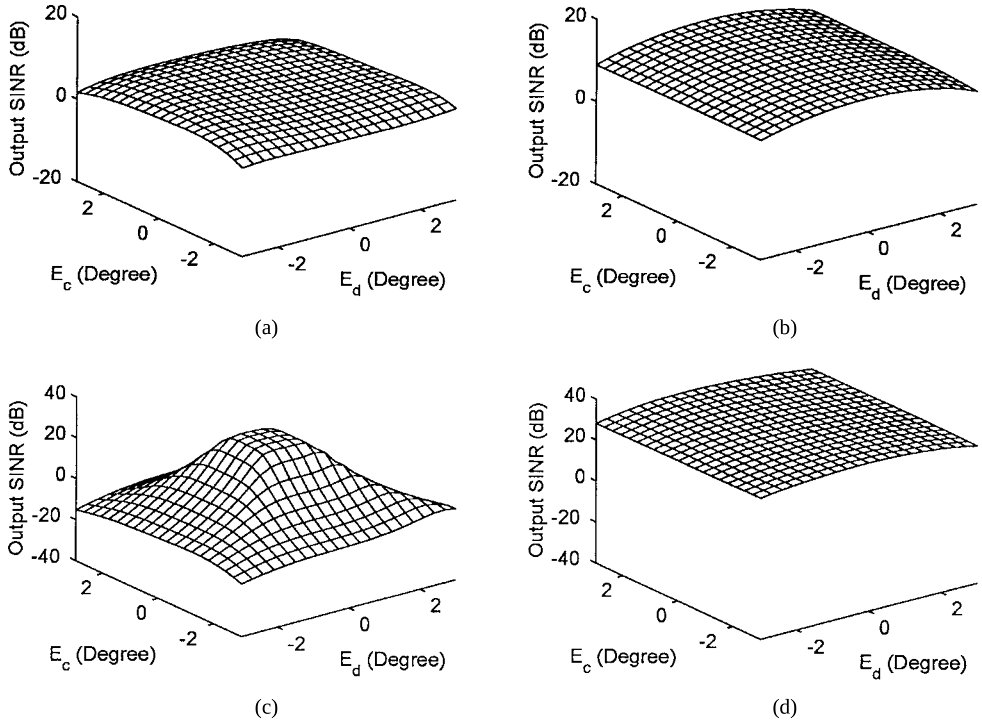

Fig. 3. Comparison of output SINR versus (E_d, E_c) for MCMV and CTMV beamformers employing second-order constraints. (a) MCMV, SNR $=0$ dB. (b) CTMV, SNR $=0$ dB. (c) MCMV, SNR $=20$ dB. (d) CTMV, SNR $=20$ dB.

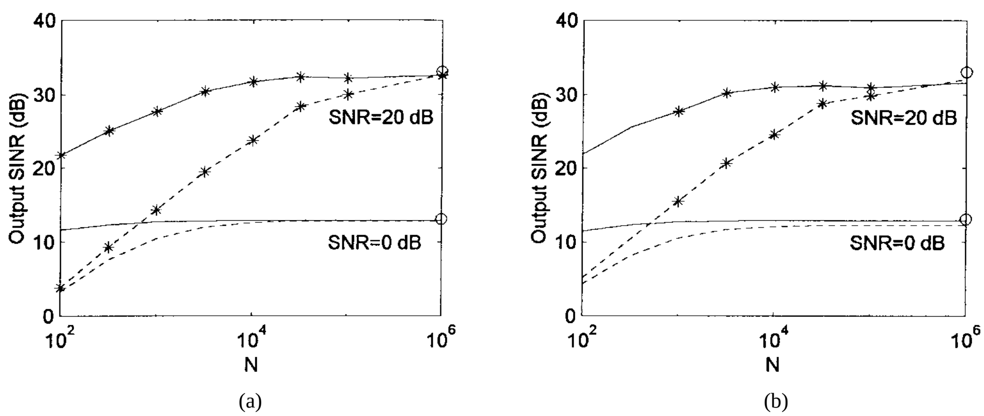

Fig. 4. Comparison of convergence behaviors of CTMV and MCMV beamformers. $E_d = E_c = 0°$. (a) Zeroth-order constraints. (b) Second-order constraints. Solid line with asterisk: CTMV, SNR $=20$ dB. Dashed line with asterisk: MCMV, SNR $=20$ dB. Solid line: CTMV, SNR $=0$ dB. Dashed line: MCMV, SNR $=0$ dB. Small circles: optimum SINR.

optimum SINR (marked by small circles), especially at high SNR. The poor performance of the MCMV beamformer with insufficient data is mainly due to the desired signal cancellation phenomenon, which, in turn, is incurred with the errors in $\hat{\boldsymbol{R}}_{xx}$ [8]. Employing the second-order constraints does not seem to help much. However, by working with a desired signal suppressing transformation for the CTMV beamformer, this problem is greatly alleviated.

Finally, to gain further insights, the directional gains (in decibels) for the desired source, coherent interferer, and uncorrelated interferer, denoted as G_d, G_c, and G_u, respectively, are listed in Table I for four different combinations of (E_d, E_c) with SNR $=20$ dB. The corresponding output SINR values are also included for reference. Note that the optimum SINR achievable in this case is 32.9 dB. First, observing the number in (a) obtained with the zeroth-order constraints we see that the CTMV beamformer achieves more reliable look direction gain and better suppression for the coherent interferer than the MCMV beamformer in the presence of DOA estimation errors. The price paid is the poorer nulling for the uncorrelated interferer due to the error in the CT steering vector $\tilde{\boldsymbol{a}}(\theta_3)$. Fortunately, the degradation does not affect the output SINR. Except for the ideal case of $(E_d, E_c) = (0°, 0°)$, the MCMV beamformer breaks down due to desired signal cancellation. Next, by using the second-order constraints, the MCMV beamformer improves significantly to avoid performance breakdown in the presence of DOA estimation errors, though the output SINR values are still far from satisfactory. On the other hand, the CTMV beamformer performs quite reliably, with sufficient nulling for both interferers, regardless

TABLE I
COMPARISON OF DIRECTIONAL GAINS (IN DECIBELS) FOR THE DESIRED SOURCE (G_d), COHERENT INTERFERER (G_c) AND UNCORRELATED INTERFERER (G_u), AND OUTPUT SINR (SINR_o) ACHIEVED BY THE CTMV AND MCMV BEAMFORMERS WITH (E_d, E_c) AS PARAMETERS. SNR = 20 dB. (a) ZEROTH-ORDER CONSTRAINTS. (b) SECOND-ORDER CONSTRAINTS

(E_d,E_c)		(0°, 0°)	(0°, 2°)	(2°, 0°)	(2°, 2°)
CTMV	G_d (dB)	0	0	−2.2	−2.7
	G_c (dB)	−81.6	−12.8	−16.3	−11.2
	G_u (dB)	−63.4	−58.1	−56.1	−57.4
	SINR_o (dB)	32.5	29.5	27.1	24.4
MCMV	G_d (dB)	0	0	−57.8	−7.4
	G_c (dB)	$-\infty$	0	$-\infty$	−7.4
	G_u (dB)	−129.3	−111.8	−118.0	−119.4
	SINR_o (dB)	32.9	−28.3	−29.7	−34.9

(a)

(E_d,E_c)		(0°,0°)	(0°, 2°)	(2°, 0°)	(2°, 2°)
CTMV	G_d (dB)	0	0	−1.7	−1.7
	G_c (dB)	−81.6	−41.5	−49.9	−43.8
	G_u (dB)	−57.1	−59.7	−56.3	−56.2
	SINR_o (dB)	31.5	32.0	29.5	29.5
MCMV	G_d (dB)	0	0	−9.1	−6.3
	G_c (dB)	$-\infty$	−7.6	$-\infty$	−11.6
	G_u (dB)	−122.3	−100.6	−98.8	−104.5
	SINR_o (dB)	32.3	1.5	−1.3	−4.3

(b)

of the DOA estimation errors. It is noteworthy that as opposed to the degradation of the MCMV beamformer, the CTMV beamformer achieves uniformly high output SINR for all four cases.

VI. CONCLUSION

A new scheme of adaptive beamforming for combating coherent interference was presented. The scheme was developed based on a complemental transformation which can be applied to an arbitrary array configuration. The transformation, together with a noise-power estimate, yields a correlation matrix with the desired signal suppressed and the interference-plus-noise component unchanged. This results in a beamformer dealing only with the interference and noise such that the maximum SINR can be achieved without the degradation due to steering vector errors. The proposed beamformer (termed the CTMV beamformer) is superior in sensitivity to the conventional MCMV beamformer with hard nulls imposed in the directions of coherent interferers. In particular, the CTMV beamformer can be viewed as working with soft constraints for the coherent interferers to prevent them from mutually cancelling the desired signal. Performance analysis and computer simulations confirm that the CTMV beamformer exhibits much better robustness to the constraint errors and faster convergence compared to the MCMV beamformer.

REFERENCES

[1] R. A. Monzingo and T. W. Miller, *Introduction to Adaptive Arrays*. New York: Wiley, 1980.

[2] B. Widrow, K. M. Duvall, R. P. Gooch, and W. C. Newman, "Signal cancellation phenomena in adaptive antennas: Causes and cures," *IEEE Trans. Antennas Propagat.*, vol. AP-30, pp. 469–478, May 1982.

[3] A. K. Luthra, "A solution to adaptive nulling problem with a look-direction constraint in the presence of coherent jammers," *IEEE Trans. Antennas Propagat.*, vol. AP-34, pp. 702–710, May 1986.

[4] T. J. Shan and T. Kailath,"Adaptive beamforming for coherent signals and interference," *IEEE Trans. Acoust., Speech, Signal Processing*, vol. ASSP-33, pp. 527–536, June 1985.

[5] C. C. Yeh and W. D. Wang, "Coherent interference suppression by an antenna array of arbitrary geometry," *IEEE Trans. Antennas Propagat.*, vol. 37, pp. 1317–1322, Oct. 1989.

[6] A. J. Weiss and B. Friedlander, "Performance analysis of spatial smoothing with interpolated array," *IEEE Trans. Signal Processing*, vol. 41, pp. 1881–1892, May 1993.

[7] A. K. Steele, "Comparison of directional and derivative constraints for beamformers subject to multiple linear constraints," *Proc. Inst. Elect. Eng.*, vol. 130, pt. F, pp. 41–45, Feb. 1983.

[8] D. D. Feldman and L. J. Griffiths, "A projection approach for robust adaptive beamforming," *IEEE Trans. Signal Processing*, vol. 42, pp. 867–876, Apr. 1994.

[9] D. G. Luenberger, *Optimization by Vector Space Methods*. New York: Wiley, 1969, ch. 4, pp. 84–86.

[10] P. Stoica, "On estimating the noise power in array processing," *Signal Processing*, vol. 26, pp. 205–220, 1992.

[11] M. Wax and Y. Anu, "Performance analysis of the minimum variance beamformer," *IEEE Trans. Signal Processing*, vol. 44, pp. 928–937, Apr. 1996.

Ta-Sung Lee was born in Taipei, Taiwan, R.O.C., on October 20, 1960. He received the B.S. degree from National Taiwan University, Taipei, Taiwan, in 1983, the M.S. degree from the University of Wisconsin, Madison, in 1987, and the Ph.D. degree from Purdue University, West Lafayette, IN, in 1989, all in electrical engineering.

From 1987 to 1989, he was a David Ross Graduate Research Fellow at Purdue University. In 1990, he joined the Faculty of National Chiao Tung University, Hsinchu, Taiwan, where he currently holds a position as Professor in the Department of Communication Engineering. His research interests include adaptive beamforming, smart antennas for wireless communications, and sound signal processing.

Dr. Lee is a member of Phi Tau Phi.

Tsui-Tsai Lin was born in Taoyuan, Taiwan, R.O.C., on September 21, 1967. He received the B.S. degree in 1991, M.S. degree in 1993, and Ph.D. degree in 1997, all in communication engineering from National Chiao Tung University, Hsinchu, Taiwan.

In 1997, he joined the Computer and Communication Research Laboratories of Industrial Technology Research Institute (ITRI), Hsinchu, Taiwan, where he is currently involved in the development of technology of global system for mobile communications (GSM). His research interests are in adaptive arrays and mobile communications.